

We are IntechOpen, the world's leading publisher of Open Access books Built by scientists, for scientists

6,900

Open access books available

186,000

International authors and editors

200M

Downloads

Our authors are among the

154

Countries delivered to

TOP 1%

most cited scientists

12.2%

Contributors from top 500 universities



WEB OF SCIENCE™

Selection of our books indexed in the Book Citation Index
in Web of Science™ Core Collection (BKCI)

Interested in publishing with us?
Contact book.department@intechopen.com

Numbers displayed above are based on latest data collected.
For more information visit www.intechopen.com



Experimental Study of Porous Silicon Films

Salah Rahmouni and Lilia Zighed

Additional information is available at the end of the chapter

<http://dx.doi.org/10.5772/intechopen.74479>

Abstract

In the present study, porous silicon films were prepared on N- and P-type silicon wafer (100) crystallographic orientations. We have investigated the influence of the different anodization parameters and silicon wafers on the properties of the obtained porous silicon layer such as thickness and porosity. The reflectance measurement of the prepared samples has presented reduction of reflection due to the porous layers and suggests the antireflective character of the realized porous layer.

Keywords: porous silicon, antireflective coating, electrochemical anodization, solar cell, HF

1. Introduction

The increasing need of energy induces a strong greenhouse gas emission since energy production is mainly achieved by fossil fuel combustion. This gas excess has a harmful effect on the life on earth. To satisfy the increasing demand in energy, without altering our environment, it is indispensable to recourse to clean and renewable energies. Solar energy is one of the most promising renewable energy sources. Photovoltaic electricity is obtained by direct transformation of sunlight to electricity by means of solar cell. During the last few decades, photovoltaic market has an increasable progress. This leads to a growing research activity based on new materials and devices for obtaining more efficient solar cells with low cost. The reduction of optical energy losses is one of the most important factors in manufacturing high-efficiency silicon solar cells [1]. After its discovery in 1956 by Uhler [2], porous silicon

has attracted more intentions due to their interesting properties like antireflective coating, improving photovoltaic conversion efficiency [3–7]. Furthermore, its important specific surface has attracted earlier a technological interest in photoluminescence at room temperature and electroluminescence [8].

Electrochemical etching is considered as the most appropriate method to produce homogeneous porous silicon [9, 10]. The aim of this study is the comparison between two types of porous silicon (P and N) generated with the above electrochemical method in order to see the effect of several experimental parameters (current density, anodization time, and hydrofluoric acid “HF” concentration) on the porosity, thickness, and antireflective activity, respectively.

The present work deals with the production of porous silicon by electrochemical way, to use it as antireflective coating for solar cell. We have studied the influence of the experimental parameters such as anodization time, current, and substrate type N or P on the final porous layer thickness, porosity, and antireflective activity.

2. Experimental details

PS layer was fabricated on P-type and N-type single crystal silicon wafers with a (100) crystallographic orientation and a resistivity of 3–5 Ωcm . After a standard cleaning process, a good ohmic aluminum contact has been evaporated onto the back of samples. Anodization was then performed in a [2, 3] volume ratio of a solution composed of 40% HF and 98% ethanol.

The electrochemical anodization of silicon is achieved by a homemade system; the experimental setup is presented in **Figure 1**.

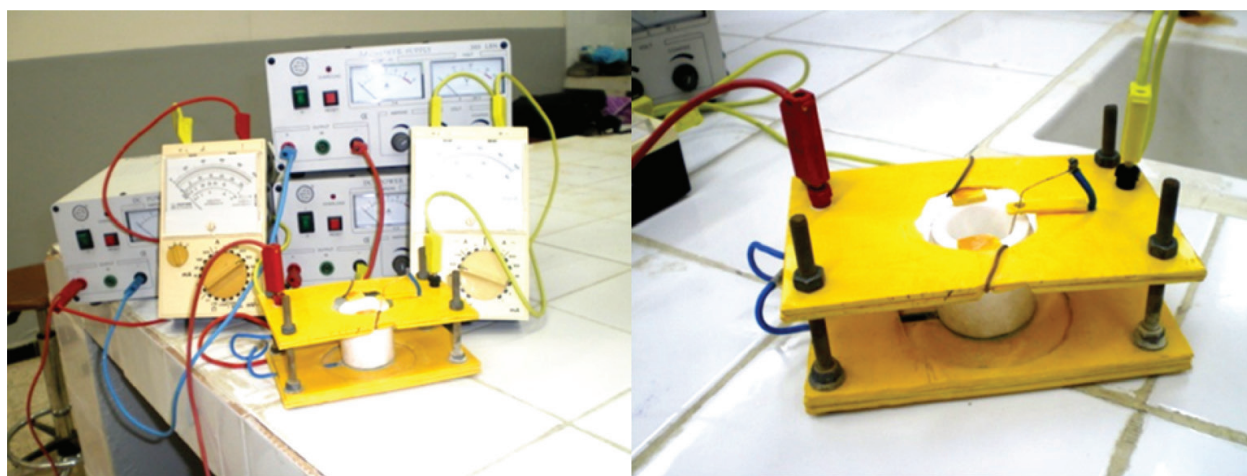


Figure 1. Photograph of used experimental device for Si substrate anodization.

3. Experimental protocol

3.1. Design of the anodizing platform

In order to produce porous silicon layers with a diameter of ≈ 10 mm, we proceeded the design of an anodizing nacelle with a circular opening.

Figure 2 shows the schematic diagram of the anodizing device consisting of the anodizing nacelle, along with a stabilized power supply that provides a constant current. This anodizing cell uses a metal electrical contact on the back side of the silicon wafer, isolated from the HF/ethanol solution by an HF inert O-ring. Thus, only the front face is exposed to the electrolyte attack. Obviously, the diameter of the O-ring controls the diameter of the obtained porous silicon stain, which remains valid when the edge effects are neglected.

3.2. Preparation of the substrate

The porous silicon samples were made by using the electrochemical anodizing method. This method is widely used, providing homogeneous porous layers, the porosity and the thickness of the elaborate layer are so controllable.

The silicon (Si) substrates used are monocrystalline, oriented (100), and (111) P and N type. Before anodization process, and in order to ensure a good electrical contact, an aluminum plate is placed on the back face of the substrate.

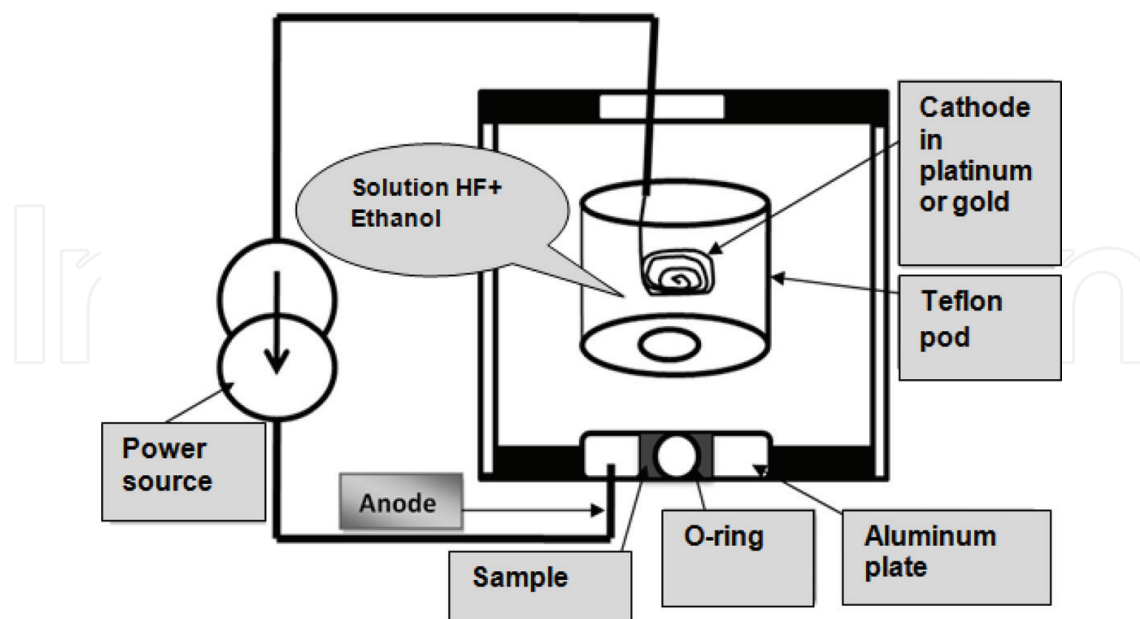


Figure 2. Diagram of the porous silicon manufacturing system.

3.3. Cleaning protocol

Before preparation, the samples must be well cleaned accordingly to the following protocol presented (**Figure 3**) in the synoptic diagram of the cleaning protocol.

3.4. Anodizing

3.4.1. Mounting of elaboration

The porous silicon layers (PS) are obtained after electrochemical etching in solution of hydro-fluoric acid (HF) and ethanol (C₂H₅OH). We note that the role of ethanol is to standardize the porous layer and to minimize the formation of hydrogen bubbles at the surface, which homogenizes the porous layer [11, 12].

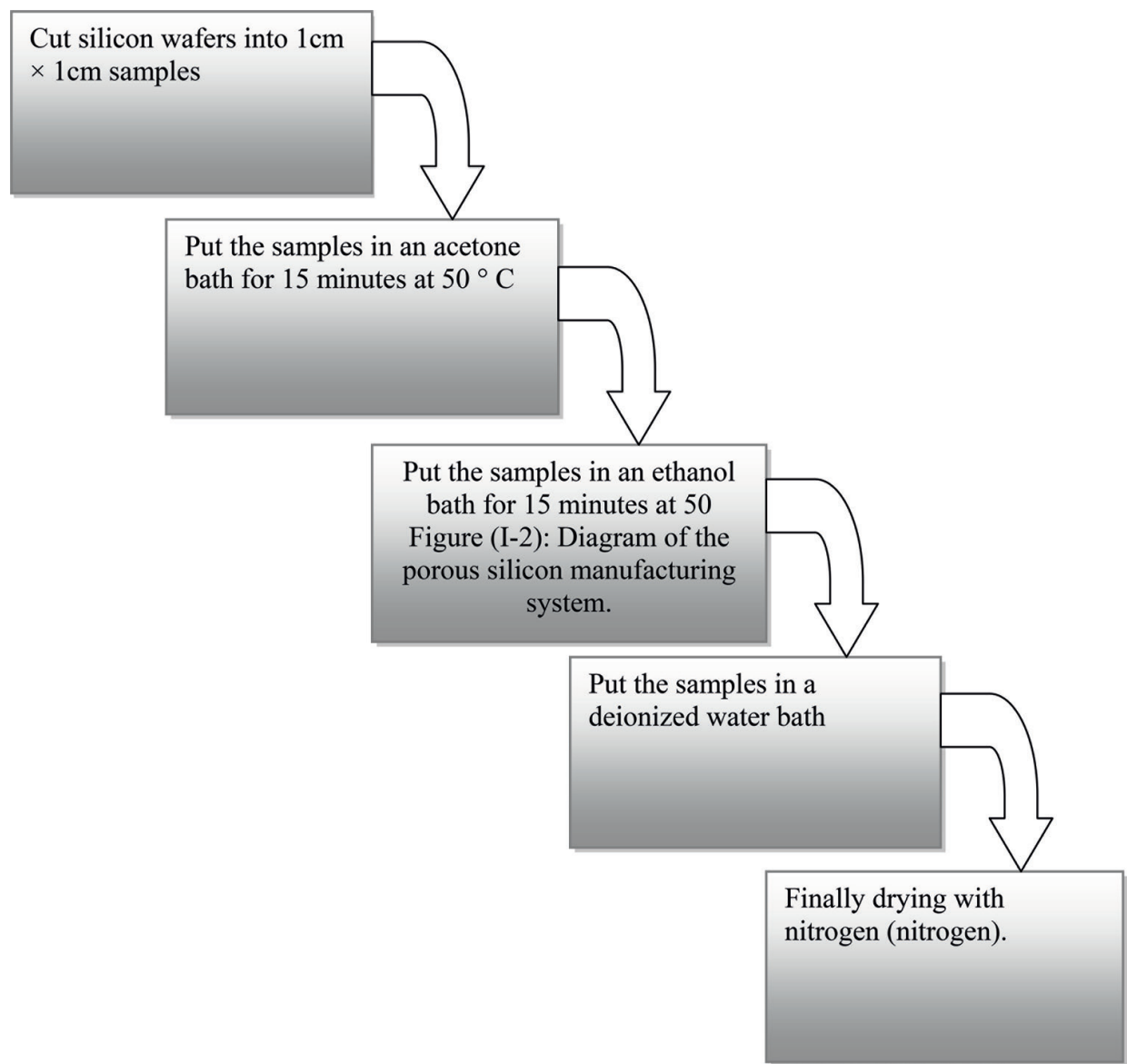


Figure 3. Synoptic diagram of the cleaning protocol.

The electrochemical dissolution is carried out in an impermeable material known as Teflon cell, by using the electrolyte of hydrofluoric acid solution having a high corrosive property. The cathode used in our electrochemical reactions was a circular gold or platinum grid. The Si substrate playing the role of anode is placed vertically against a circular orifice having a surface of 0.64 cm² in contact with the electrolyte. The shape of the cathode makes it possible to ensure a uniform distribution of the electric field lines, and subsequently the electrochemical etching of the substrate becomes homogeneous (see **Figure 2**). To ensure the reproducibility of the morphology of the layers and to control the porosity and the thickness, the constant-current dissolution which circulates between the two electrodes has been performed.

3.4.2. Anodizing parameters

Electrolyte concentration, current density, type and doping rate of silicon, electrolyte temperature, and illumination [12–16] are essential parameters for production of porous silicon.

- i. Type and doping rate: A nano- and macroporous PS distribution was carried out on P- and N-type Si substrates. The spongy structure obtained is composed of nanocrystallites with sizes varied between 1 and 5 nm, separated by nanopores of the same type dimensions, for P-type substrates [11, 17–19], and macropores for N-type substrates [20, 21].
- ii. Composition of the electrolyte: The electrolyte is composed of 40% HF and ethanol. Vial and Derrien [22] showed that porosity decreases with increasing concentration at a constant current density. In our case, we used several volume ratios for the different elaborations.

Silicon quality	Samples	Anodizing current density (mA/cm ²)	Anodizing time (s)	Solution volume ratio (HF:C ₂ H ₅ OH)
Solar	A1(P100)	15	60	1:1
	A2(P100)	15	120	1:1
	A3(P100)	15	180	1:1
	A4(P100)	15	240	1:1
Solar	B1(P100)	5	180	1:1
	B2(P100)	10	180	1:1
	B3(P100)	15	180	1:1
	B4(P100)	20	180	1:1
Electronic	C1(P100)	30	120	3:2
	C2(P100)	10, 15, 18, 20, 30, 35, 54, 70	60, 120, 180, 240, 300, 360	2:3
	C3(N100)	10, 18, 30, 35, 54, 70, 214	360	2:3, 1:3
	C4(N111)	10, 20, 35, 106, 140	60, 120, 180, 240, 300, 360	2:3
			60, 120, 180, 240 300, 360	

Table 1. The conditions of anodization of the used substrates.

iii. Anodizing current: Note that the anodizing current and the concentration of the electrolyte have opposite effects in the formation of pores [23]. For a given concentration of the electrolyte, the porosity increases as a function of the current density. In our case, the anodizing conditions are detailed in **Table 1**.

Table 1 shows detailed data of the training conditions relating to the various samples of porous silicon produced.

4. Properties of substrates

In our work, we have used substrates of monocrystalline silicon types N and P, whose characteristics are presented in **Table 2** below.

Substrates	Dopant	Resistivity Ωcm	Orientation
N	Phosphore	(5–7)	100
N	Phosphore	(3–5)	111
P	Bore	(3–5)	100
P	Bore	(0.01–2)	100

Table 2. Characteristic of the used substrates.

5. The I (V) characteristic

The (I-V) characteristic of the electrolyte semiconductor junction depends on the nature of the semiconductor substrate as well as the ionic and molecular species present in the electrolyte. The application of an electrical potential to the silicon bathed in a solution of HF (see **Figure 1**) induces a measurable current circulating through the system.

At the silicon/electrolyte interface, the electronic charge carriers in the silicon of ionic form pass into the solution. This conversion is carried out by means of a redox reaction.

The value of the applied potential and the reaction taking place at the interface influences on the formation of porous silicon.

For the study of the I (V) characteristic the electrolytic solution which we used is formed of the following volume ratio fractions: 2 HF:3 ethanol.

In our experimental work, we used absolute ethanol and a hydrofluoric acid concentration of 40%. The previous proportions, i.e., 2 HF:3 ethanol, reduce the concentration [HF] in the resulting electrolyte to 16%.

Figure 4 shows the I (V) characteristic of the electrochemical anodization of a sample of monocrystalline silicon types (a) N (100), (b) N (111), and (c) P (100).

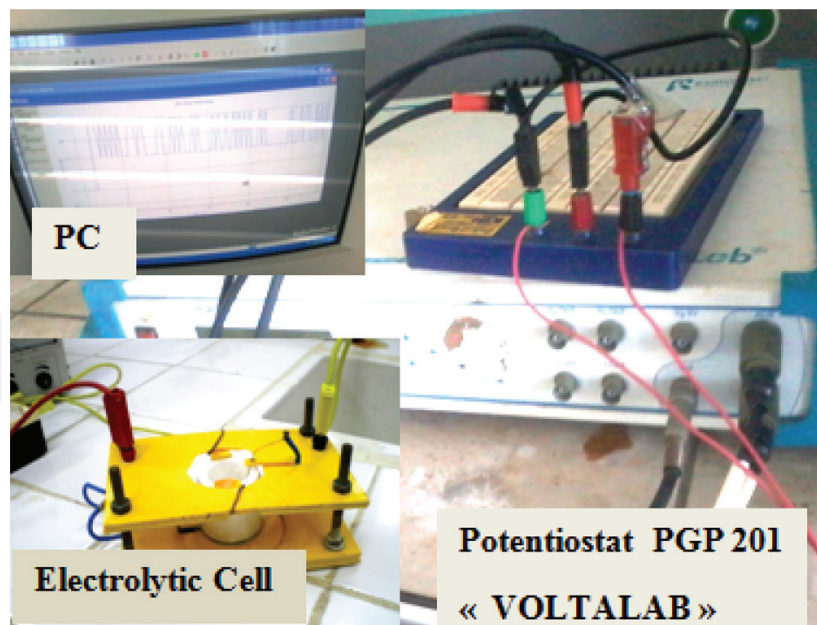


Figure 4. Mounting used for sample preparation.

There are three areas that characterize the anodizing process, the $I(V)$ curves, showing the existence of an I_{ps} current delineating the formation and electropolishing zones.

5.1. Porosification zone ($I < I_{ps}$)

In our work and using N-type substrates, the obtained $I(V)$ characteristics show a possibility to prepare porous silicon with high currents. The porosification zone remains the same with somewhat high values of current. This is due to the high value of the resistivity on the one hand and also the nature of the substrates on the other hand (N type), in addition to the fact that the experiment takes place in the dark and at room temperature. Under these conditions, the intrinsic concentration of holes is too low to form pores, so it is necessary to generate holes by applying a high potential [24]. The layers are obtained using the following conditions.

In the case of the P-type substrate, the concentration of the holes on the surface is greater than that of the fluorine ions, so anodization leads to the formation of pores.

The J_{ps} depends mostly on the composition of the HF solution in ethanol and little on the substrate.

5.2. Electropolishing zone ($I > I_{ps}$)

According to the literature, this zone appears when the anode potentials are high [25]. For N-type substrates, when $I > I_{sp}$ the limiting factor becomes the diffusion of the ionic species in the electrolyte, the holes then in excess at the bottom of the pores penetrate the porous structure which gradually generates the total dissolution of the latter [26].

In the case of P-type substrate, the density of holes on the silicon surface is important. Etching is limited by the diffusion of F-fluorine ions.

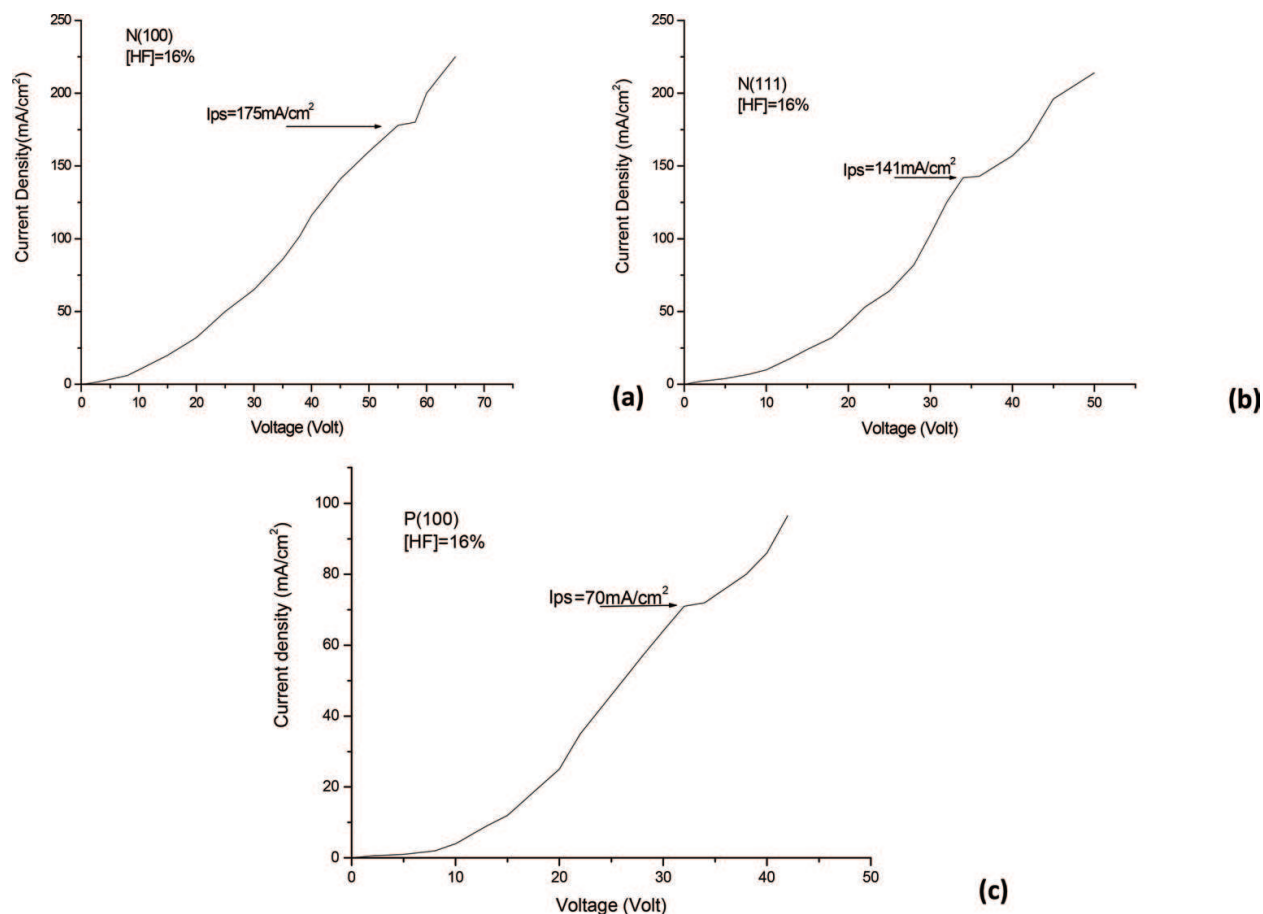


Figure 5. I (V) characteristic of silicon substrate electrochemical anodization types (a) N (100), (b) N (111), and (c) P (100).

The latter are attracted by the electric field located on the surface defects; the engraving in these places will be predominant tending to smooth the surface.

According to Ozanam and Chazalviel, electropolishing exists with an oxide layer that forms on the silicon surface for $I > I_{sp}$ currents [25].

5.3. Transition zone

If the anode potentials are at an intermediate level, there is a so-called transition zone. Since the morphology of the resulting surface is porous in nature, pore size increases rapidly with increasing potentials, leading to electropolishing of the surface.

This zone is characterized by a peak current corresponding to the formation of an oxide layer necessary for the surface electropolishing reaction [27].

6. Measurement of the thickness

6.1. Influence of anodizing time on thickness

In regard to the thickness measurement by profilometry, we studied the influence of the various anodizing parameters.

The samples studied are obtained using an electrolytic solution of a concentration

[HF] = 16%, in which the current density j is 35 mA/cm², for the silicon P (100). For silicon N (100), we used a current density of 54 mA/cm².

From **Figure 6** the thickness of the porous layer increases linearly with the anodizing time, for a current density and a given RF concentration. The number of dissolved silicon atoms is therefore directly proportional to the amount of charge exchanged ($Q = j \times$ the dissolution time) showing that the dissolution valence is invariant in time.

In the limit of the porous silicon formation regime, similar behaviors are observed, whatever the anodization current and the HF concentration [25–28].

6.2. Influence of the current density on the thickness

To know the influence of the current density on the thickness of the porous layer and on the etch rate, we set the attack time at 2 min for the three types of silicon that are available to us. For silicon types N (111) and P (100), we used an electrolytic solution concentrated at 16% HF. For the substrate type N (100), we have the same solution concentrated at 17.1%. The results obtained are presented by the graphs of **Figure 7**.

Figure 7 shows the variation of the thickness of the porous layer and the etch rate versus anodization current density for silicon substrates: (a) type N (111), (b) type P (100), and (c) type N (100). We note that the thicknesses of the obtained layers and the etch rates are increasing in a function of the current density [28].

For the N-type substrate (111), the thickness (the etch rate) of the porous layers increases linearly from 1.4 μm (0.7 $\mu\text{m}/\text{min}$) for j varying from 18 mA/cm² up to 106 mA/cm². For N- (100)

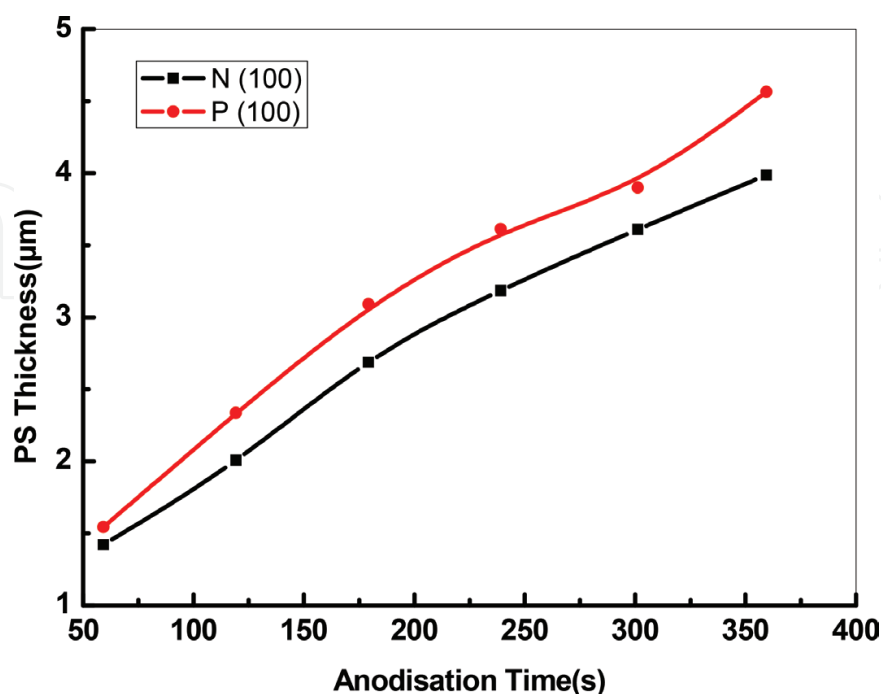


Figure 6. Variation of PS layer thickness as a function of anodization time in N-type Si (100) and P-type Si (100) substrates. The used conditions are [HF] = 16% and current density of 35 mA/cm².

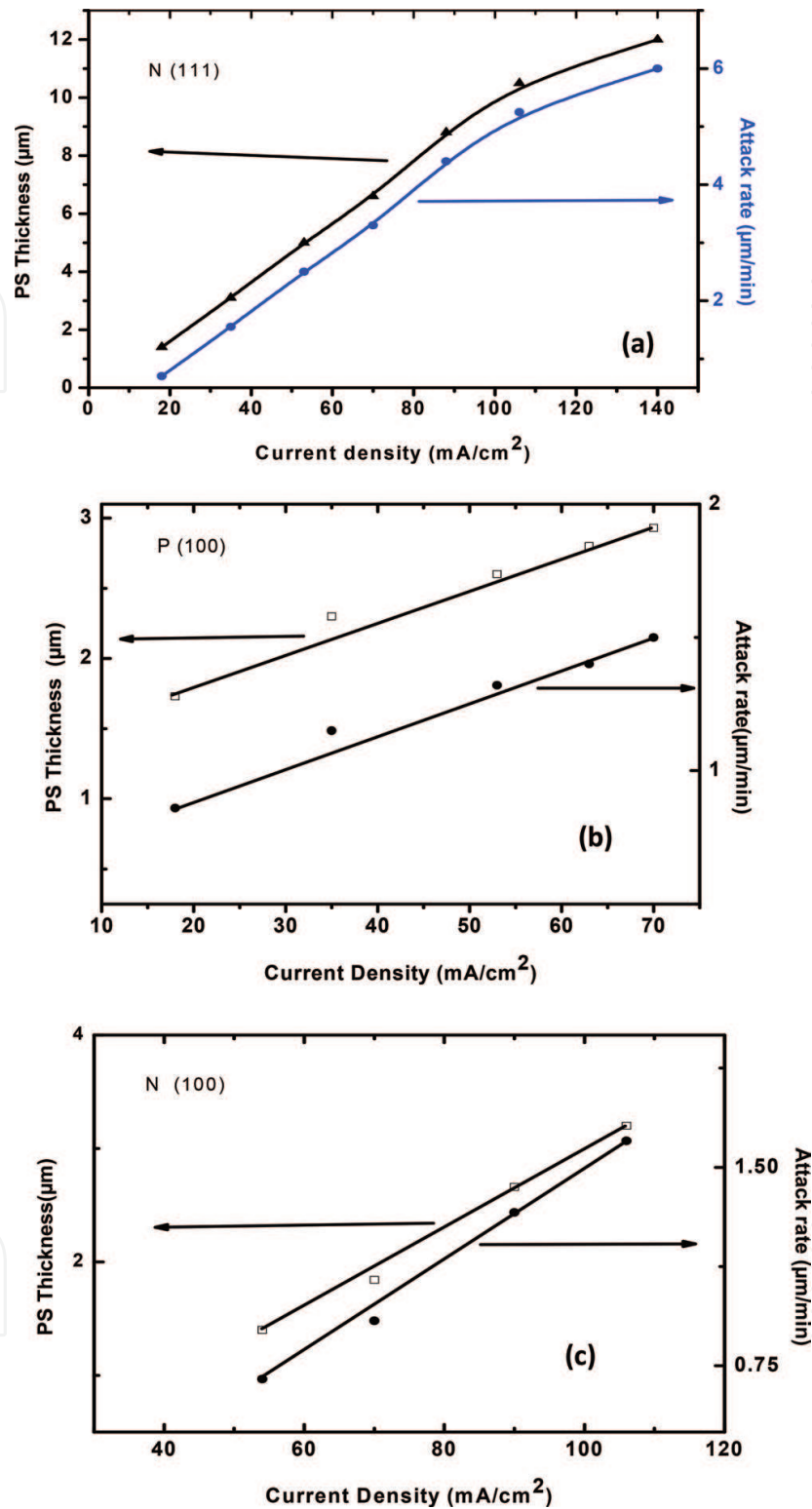


Figure 7. PS layers thickness variation and etch rate variation versus current density in (a) N-type Si (100) and (b) P-type Si (100) wafers.

and P- (100) type substrates, we note that the variation in thickness (etch rate) versus current density is linear.

For type N (100), the variation increases from $1.4 \mu\text{m}$ ($0.7 \mu\text{m}/\text{min}$) for $j = 54 \text{ mA}/\text{cm}^2$ to $3.19 \mu\text{m}$ ($1.68 \mu\text{m}/\text{min}$) for $j = 106 \text{ mA}/\text{cm}^2$. In the case of the substrate type P (100), the

variation increases from 1.7 μm (0.12 $\mu\text{m}/\text{min}$) for $j = 18 \text{ mA}/\text{cm}^2$ up to 2.9 μm (1 $\mu\text{m}/\text{min}$) for $j = 70 \text{ mA}/\text{cm}^2$.

7. Determination of porosity

One of the important features of porous silicon is the degree of porosity, i.e., the percentage of void in the porous silicon volume [29]. In our work, the determination of the porosity of the studied samples was carried out by the gravimetric method.

In our study, the porous silicon layers are prepared at room temperature and without illumination. The electrolytic solution used is prepared from 40% concentrated hydrofluoric acid diluted in absolute ethanol. To know the variation of the porosity as a function of the current density, we fixed the anodization time at 2 min.

7.1. Influence of current density on porosity

Our study is made on silicon P (100) and N (100).

The variations in porosity as a function of the current density of the samples prepared are shown in **Figure 8**.

Figure 8 shows that porosity increases as a function of current density [28]. It increases from 33% for a current density equal to 18 mA/cm^2 in the case of silicon type P (100), up to 63% for $j = 70 \text{ mA}/\text{cm}^2$.

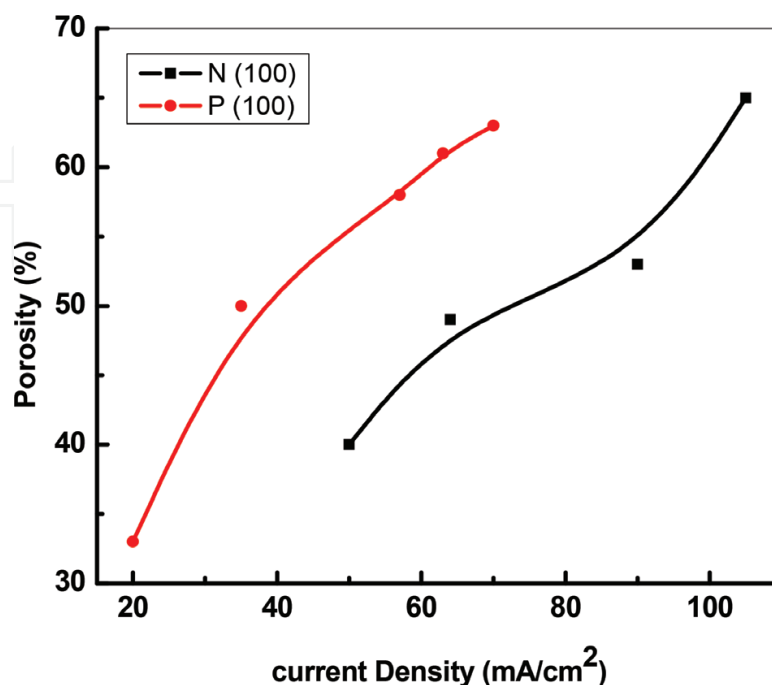


Figure 8. PS layers' porosity variation as a function of current density in (a) N-type Si (100) and (b) P-type Si (100) wafers. The used conditions are $[\text{HF}] = 16\%$ and current density of 35 mA/cm^2 .

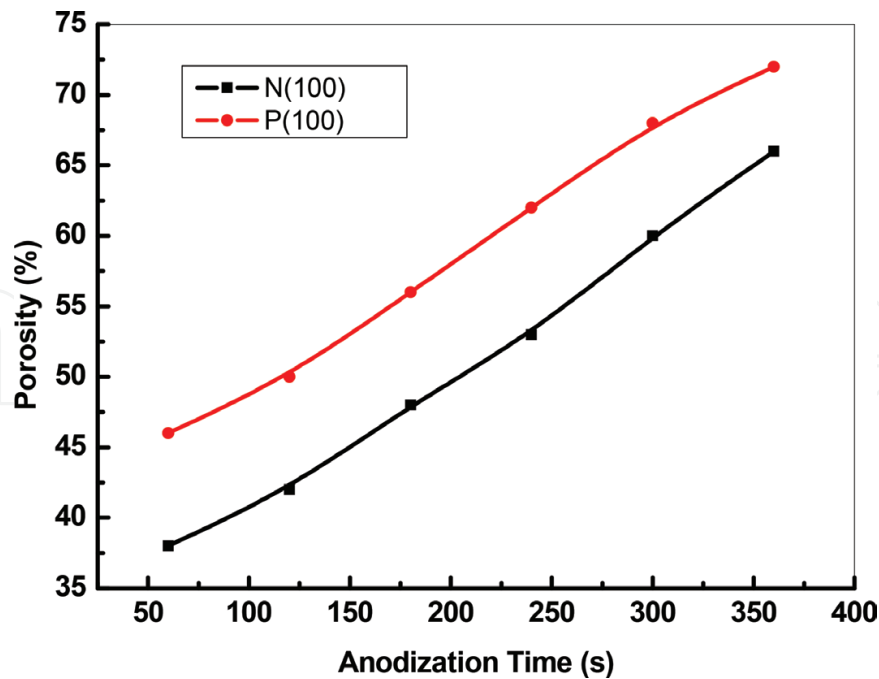


Figure 9. Porosity variation as a function anodization time measured in both Si substrates. The used conditions are [HF] = 16% and current density of 35 mA/cm².

For the N-type substrate (100), we obtained a variable porosity between 40 and 65% for a current density between 50 and 106 mA/cm².

7.2. Influence of anodization time on porosity

To know the influence of the anodization time on the porosity, we fixed the current density at $j = 35 \text{ mA/cm}^2$. The concentration of [HF] = 16% in the electrolyte, and we varied the anodizing time. We obtained the curves of **Figure 9**.

In 6.1, we concluded that the thickness of the porous layer varies linearly with anodization time; from **Figure 9**, we note that the porosity also varies almost linearly over time in a function of the anodizing time. It ranges from 38 to 64% for a sample type N silicon (100), for anodizing time from 60 to 360 s, respectively. This porosity increases from 45% up to 71% for an anodizing time from 60 to 360 s for the P-type silicon sample (100).

8. Reflectivity measurement

We measured the reflection factor of two samples obtained after electrochemical anodization of N (100) and P (100) silicon substrates. The formation conditions as well as the thicknesses and porosities for the two samples are summarized in **Table 3**.

The obtained spectra are represented by **Figure 10**.

PS layers are generally used as antireflective layer in front of solar cells to reduce the light losses. The total reflectance was measured within the 400–1100 nm wavelength range

Sample	[HF] %	j (mA/cm ²)	t (s)	d (nm)	P %
N (100)	16	54	360	3700	68.75
P (100)	16	70	120	2660	55

Table 3. Anodization conditions and physical parameters of Si samples used for reflectance measurement.

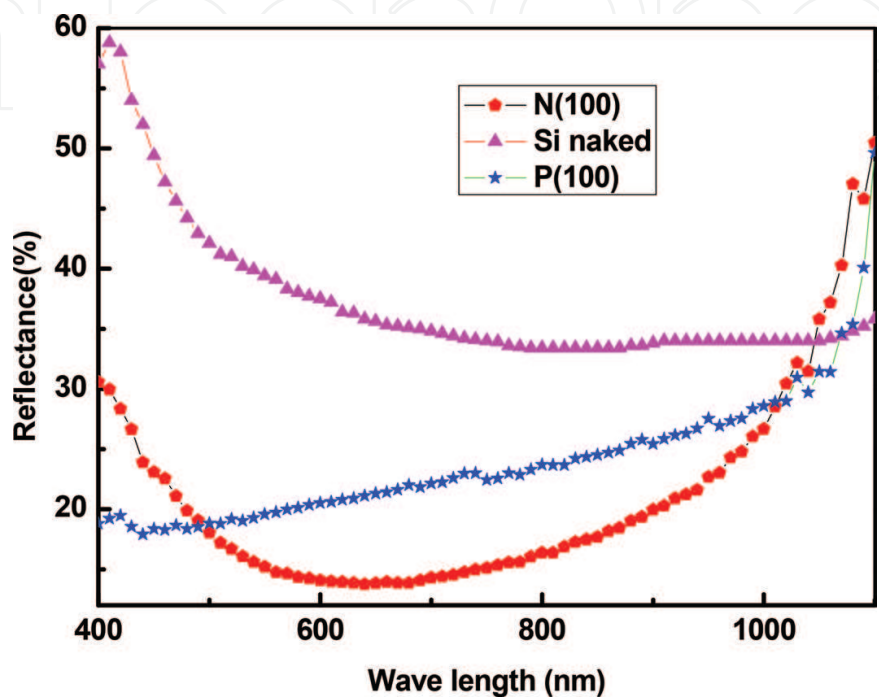


Figure 10. Variation of reflection coefficient as a function of the incident light wavelength measured in naked Si sample used as reference and N-type and P-type Si with PS layer.

with an integrating sphere, as described in **Figure 10**, where we have reported the reflection coefficient of the three studied samples: the reference Si naked (N-type) that does not undergo any chemical etching and N-type and P-type Si with porous layer. The conditions used here, such as thickness and relative porosities to the two Si samples, are summarized in **Table 1**. From **Figures 1–10**, one can deduce that the formation of PS layer reduces drastically the sample reflection coefficient due to the light entrapment in the formed pores. The reduction of losses by reflection caused by porous silicon layers indicates the antireflective character of this film type. This result agrees with what is returned in the literature [6, 8].

The antireflective activity is more significant in the N-type Si > as example for the 600 nm wavelength, the measured reflection coefficients are, respectively, 13, 20, and 37% for N-type, P-type, and naked Si substrates.

This is due to the fact that in the N type, pores have a smaller size and are uniformly distributed on the sample surface in contrary to P-type Si, where the pores are larger and spatially localized in tranches.

9. Conclusion

In the present work, we have investigated the influence of anodization time and current density upon the PS layer formation on N-type and P-type Si substrate. The formed pores in N-type Si are uniformly distributed over the sample surface with a small size, indicating an isotropic and homogenous attack of HF. However, in the case of P type, the HF etching is anisotropic; it causes the formation of large trenches composed with pores at the bottom. We have noticed that the PS layer thickness and its porosity vary linearly with the anodization time and current density. Finally, due to the pore size and distribution, we found that PS layer formed on N-type Si exhibits better antireflective activity than P-type Si, making the obtained layers important tools in the solar cell.

Author details

Salah Rahmouni^{1,2*} and Lilia Zighed³

*Address all correspondence to: rahmouni.eln@gmail.com

1 Normal High School of Technological Education (ENSET), Skikda, Algeria

2 Department of Electrical Engineering, University of 20 August 1955, Skikda, Algeria

3 Laboratory of Chemical Engineering and Environment, University of 20 August 1955, Skikda, Algeria

References

- [1] Lipinski M, Panek P, Swiatek Z, Beltowska E, Ciach RS. Double porous silicon layer on multi-crystalline Si for photovoltaic application. *Solar Energy Materials & Solar Cells*. 2002;**72**:271-276. DOI: [https://doi.org/10.1016/S0927-0248\(01\)00174-X](https://doi.org/10.1016/S0927-0248(01)00174-X)
- [2] Uhler A. Electrolytic shaping of germanium and silicon. *Bell System Technical Journal*. 1956;**35**:333. DOI: 10.1002/j.1538-7305.1956.tb02385.x
- [3] Menna P, Di Francia G, Ferrara VLA. Porous silicon in solar cells: A review and a description of its application as an AR coating. *Solar Energy Materials & Solar Cells*. 1995;**37**:13-24. DOI: [https://doi.org/10.1016/0927-0248\(94\)00193-6](https://doi.org/10.1016/0927-0248(94)00193-6)
- [4] Lee MK, Wang YH, Chu CH. Characterization of porous silicon photovoltaic devices through rapid thermal oxidation, rapid thermal annealing and HF-dipping processes. *Solar Energy Materials & Solar Cells*. 1999;**59**:59-64. DOI: [https://doi.org/10.1016/S0927-0248\(99\)00031-8](https://doi.org/10.1016/S0927-0248(99)00031-8)
- [5] Strehlke S, Bastide S, Lévy Clement C. Optimization of porous silicon reflectance for silicon photovoltaic cells. *Solar Energy Materials & Solar Cells*. 1999;**58**:399. DOI: [https://doi.org/10.1016/S0927-0248\(99\)00016-1](https://doi.org/10.1016/S0927-0248(99)00016-1)

- [6] Strehlke S, Sarti D, Krotkus A, Grigoras K, Lévy-Clément C. The porous silicon emitter concept applied to multicrystalline silicon solar cells. *Thin Solid Films*. 1997;**297**:291-295. DOI: [https://doi.org/10.1016/S0040-6090\(96\)09368-6](https://doi.org/10.1016/S0040-6090(96)09368-6)
- [7] Bergmenn RB, Rinke TJ, Wagner TTA, Warner JH. *Solar Energy Materials & Solar Cells*. 2001;**65**:355
- [8] Canham LT. Silicon quantum wire array fabrication by electrochemical and chemical dissolution of wafers. *Applied Physics*. 1990;**57**:1046. DOI: <https://doi.org/10.1063/1.103561>
- [9] Asoh H, Arai F, Ono S. Effect of noble metal catalyst species on the morphology of macroporous silicon formed by metal-assisted chemical etching. *Electrochim Acta*. 2009;**54**:5142-5148. DOI: <https://doi.org/10.1016/j.electacta.2009.01.050>
- [10] Harraz FA, Salem AM, Mohamed BA, Kandil A, Ibrahim IA. Electrochemically deposited cobalt/platinum (Co/Pt) film into porous silicon: Structural investigation and magnetic properties. *Applied Surface Science*. 2013;**264**:391-398. DOI: [10.1016/j.apsusc.2012.10.032](https://doi.org/10.1016/j.apsusc.2012.10.032)
- [11] Bessais B, Ben Younes O, Ezzaouia H, Mliki N, Boujamil MF, Oueslati M, Bennaceur R. Morphological changes in porous silicon nanostructures: non-conventional photoluminescence shifts and correlation with optical absorption. *Journal of Luminescence*. 2000;**90**:101-109. DOI: [https://doi.org/10.1016/S0022-2313\(99\)00617-1](https://doi.org/10.1016/S0022-2313(99)00617-1)
- [12] Halimaoui A. Determination of the specific surface area of porous silicon from its etch rate in HF solutions. *Surface Science Letters*. 1994;**306**:L550-L554
- [13] Halimaoui A. Influence of wettability on anodic bias induced electroluminescence in porous silicon. *Applied Physics Letters*. 1993;**63**:1264-1266. DOI: <https://doi.org/10.1063/1.109752>
- [14] Tsybeskov L, Fauchet PM. Correlation between photoluminescence and surface species in porous silicon: Low-temperature annealing. *Applied Physics Letters*. 1994;**64**:1983. DOI: <https://doi.org/10.1063/1.111714>
- [15] Teschke O, Galembeck F, Gonçalves MC, Davanzo CU. Photoluminescence spectrum redshifting of porous silicon by a polymeric carbon layer. *Applied Letters*. 1994;**64**:3590. DOI: <https://doi.org/10.1063/1.111207>
- [16] Ono H, Gomyu H, Morosalci H, Nozaki S, Shou Y, Shimazaki M, Iwaze M, Izumi T. Effects of anodization temperature on photoluminescence from porous silicon. *Journal of the Electrochemical Society*. 1993;**140**(12):L180-L182. DOI: [10.1149/1.2221158](https://doi.org/10.1149/1.2221158)
- [17] Koyama H, Koshida N. Photo-assisted tuning of luminescence from porous silicon. *Journal of Applied Physics*. 1993;**74**:6365. DOI: <https://doi.org/10.1063/1.355160>
- [18] Lévy-Clément C, Lagoubiet A, Tomkiewicz M. Morphology of porous n-type silicon obtained by photoelectrochemical etching I. Correlations with material and etching parameters. *Journal of the Electrochemical Society*. 1994;**141**:958. DOI: [10.1149/1.2054865](https://doi.org/10.1149/1.2054865)
- [19] Cullis AG, Canham LT, Dosser OD. The structure of porous silicon revealed by electron microscopy. *Materials Research Society Symposium Proceedings*. 1992:256. DOI: <https://doi.org/10.1557/PROC-256-7>

- [20] Levy-Clement C. Porous silicon sci, Technol, les éditions de physiques springer; 1994. pp. 327-344
- [21] Chuang SF, Collins SD, Smith RL. Preferential propagation of pores during the formation of porous silicon: A transmission electron microscopy study. *Applied Physics Letters*. 1989;**55**(7):675-677. DOI: <https://doi.org/10.1063/1.101819>
- [22] Vial JC, Derrien J, editors. Porous silicon in science and technology Winter. Berlin: School Les Houches, Springer-Verlag; 1994 Les Editions de Physique, Les Ulis
- [23] Fathauer RW, George T, Ksendzov A, Vasquez RR. Visible luminescence from silicon wafers subjected to stain etches. *Applied Physics Letters*. 1992;**60**:995. DOI: 10.1063/1.106485
- [24] Levy Clement. Characteristics of porous n-type silicon obtained by photo électrochemical etching dans porous silicon science and Technology. Les éditions de physique springer; 1994. p. 329
- [25] Ozanam H, CHazalviel J-N. In-situ infrared characterization of the electrochemical dissolution of silicon in a fluoride electrolyte. *Journal of Electron Spectroscopy and Related Phenomena*. 1993;**64/65**:395-402
- [26] Lerondel G. Propagation de la lumière dans le silicium poreux application photonique. P (9-13-15) Thèse de doctorat université joseph Fourier –Gronoble I; 1997
- [27] Roussel P. Micro capteur de conductivité thermique sur caissons épais de silicium poreux pour la mesure de la microcirculation sanguine. Thèse Institut national des sciences Appliquées de Lyon; 1999
- [28] Halimaoui A. Porous silicon material processing properties and Technology Les éditions de physique. Vol. 1. Springer; 1994. pp. 33-52
- [29] Setzu S. Réalisation et étude de structure a modulation d'indice optique en silicium poreux, Thèse de doctorat Grenoble I; 1999

IntechOpen